Measurement of Differences between J/ψ and ψ' Suppression in p-A Collisions

M. J. Leitch,[6] W. M. Lee,[4] M. E. Beddo,[7] C. N. Brown,[3] T. A. Carey,[6] T. H. Chang,[7,*] W. E. Cooper,[3] C. A. Gagliardi,[9] G. T. Garvey,[6] D. F. Geesaman,[2] E. A. Hawker,[9,6] X. C. He,[4] L. D. Isenhower,[1] D. M. Kaplan,[5] S. B. Kaufman,[2] D. D. Koetke,[10] P. L. McGaughey,[6] J. M. Moss,[6] B. A. Mueller,[2] V. Papavassiliou,[7] J. C. Peng,[6] G. Petitt,[4] P. E. Reimer,[6,2] M. E. Sadler,[1] W. E. Sondheim,[6] P. W. Stankus,[8] R. S. Towell,[1,6] R. E. Tribble,[9] M. A. Vasiliev,[9,†] J. C. Webb,[7] J. L. Willis,[1] and G. R. Young[8]

(FNAL E866/NuSea Collaboration)

[1]*Abilene Christian University, Abilene, Texas 79699*
[2]*Argonne National Laboratory, Argonne, Illinois 60439*
[3]*Fermi National Accelerator Laboratory, Batavia, Illinois 60510*
[4]*Georgia State University, Atlanta, Georgia 30303*
[5]*Illinois Institute of Technology, Chicago, Illinois 60616*
[6]*Los Alamos National Laboratory, Los Alamos, New Mexico 87545*
[7]*New Mexico State University, Las Cruces, New Mexico 88003*
[8]*Oak Ridge National Laboratory, Oak Ridge, Tennessee 37831*
[9]*Texas A & M University, College Station, Texas 77843*
[10]*Valparaiso University, Valparaiso, Indiana 46383*

(Received 9 September 1999; revised manuscript received 17 December 1999)

Measurements of the suppression of the yield per nucleon of J/ψ and ψ' production for 800 GeV/c protons incident on heavy nuclear targets, relative to light nuclear targets, have been made with very broad coverage in x_F and p_T. The observed suppression is smallest at x_F values of 0.25 and below, and increases at larger values of x_F. It is also strongest at small p_T. Substantial differences between ψ' and J/ψ production are observed for the first time in p-A collisions. The suppression for ψ' production is stronger than that for J/ψ for x_F near zero, but becomes comparable to that for J/ψ for $x_F > 0.6$.

PACS numbers: 24.85.+p, 13.85.Qk, 14.40.Lb, 14.65.Dw

Strong suppression of the yield per nucleon of heavy vector mesons produced in heavy nuclei relative to that in light nuclei has been observed in proton and pion-nucleus collisions [1–6]. Similar effects have also been observed in heavy-ion collisions [7]. This suppression exhibits strong kinematic dependences, especially with Feynman-x (x_F) and transverse momentum (p_T) of the produced vector meson. Since the suppression of heavy vector meson production in heavy-ion collisions is predicted to be an important signature for the formation of the quark-gluon plasma (QGP), it is important to understand the mechanisms that can produce similar effects in the absence of a QGP. These mechanisms can be studied in proton-nucleus production of vector mesons where no QGP is presumed to occur. Many effects have been considered [8–11] in attempting to describe the observed proton-induced charmonium yields from nuclear targets, e.g., absorption, parton energy loss, shadowing, and feed-down from higher mass resonances, but it is clear that no adequate understanding of the problem has been achieved. Even the absolute cross sections are poorly understood due to poor knowledge of the production mechanism, and most models ignore or use naive pictures of the space-time evolution of the $c\bar{c}$ pair. Recognizing that the production and suppression mechanisms can be identified by their strong kinematic dependences, it is crucial to have new data with broad kinematic coverage to challenge comprehensive descriptions of charmonium production in nuclei.

Here we report new high statistics measurements made in Fermilab E866/NuSea of the nuclear dependence of J/ψ and ψ' production for proton-nucleus collisions on Be, Fe, and W targets. Over 3×10^6 J/ψ's and 10^5 ψ''s with x_F between -0.10 and 0.93 and p_T up to 4 GeV/c were observed. Previous measurements in E772 [1] and E789 [2,3] have suffered from limited p_T acceptance and limited statistics at larger values of x_F, both of which are greatly extended in these new data.

E866/NuSea used a 3-dipole magnet pair spectrometer employed in previous experiments (E605 [12], E772, and E789), modified by the addition of new drift chambers and hodoscopes with larger acceptance at the first tracking station and a new trigger system [13]. This spectrometer was also used for other measurements in E866/NuSea [14,15]. An 800 GeV/c extracted proton beam of up to 6×10^{11} protons per 20 s spill bombarded the targets used in these measurements. A rotating wheel which was located upstream of either the first or second magnet held thin solid targets of Be, Fe, and W with thicknesses corresponding to between 3% and 19% of an interaction length. After passing through the target, the remaining beam was absorbed in a copper beam dump located inside the large second magnet. Following the beam dump was a 13.4 interaction length absorber wall which filled the entire aperture of the magnet, eliminated hadrons, and assured that only muons traversed the spectrometer's detectors. These muons were then tracked through a series of detector stations composed

 0031-9007/00/84(15)/3256(5)$15.00

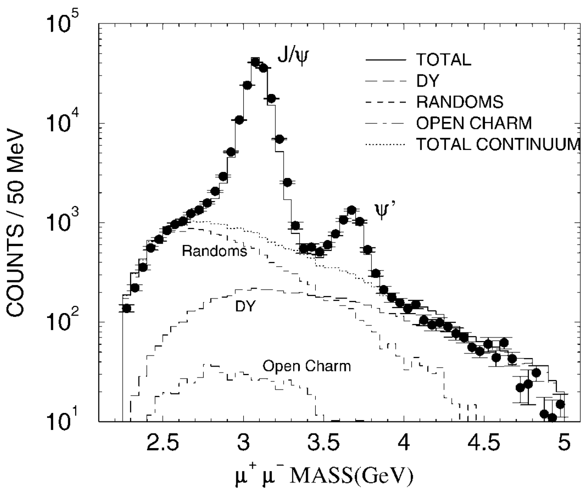

FIG. 1. Fit to the mass spectrum for the Be target in the x_F range from 0.00 to 0.05. Components in the fit are J/ψ, ψ', Drell-Yan (long-dashed), randoms (short-dashed), and open charm (dot-dashed). The solid curve represents the total of all fitted line shapes, and the dotted curve represents the continuum which is the sum of the Drell-Yan, randoms, and open charm.

of drift chambers, hodoscopes, and proportional tubes. Because of improvements in the trigger system, the coverage in p_T was much broader than in previous experiments with this spectrometer (e.g., E772), extending to over 4 GeV$/c$. Beam intensity was monitored using secondary-emission detectors.

Three magnetic field and target location configurations were used to span the full range in x_F: small x_F (SXF, $-0.1 \leq x_F \leq 0.3$), intermediate x_F (IXF, $0.2 \leq x_F \leq 0.6$), and large x_F (LXF, $0.3 \leq x_F \leq 0.93$). Detailed Monte Carlo simulations of the J/ψ and ψ' peaks and of the Drell-Yan continuum were used to generate line shapes in each bin in x_F or in p_T. For the Drell-Yan calculations we use Martin-Roberts-Stirling-Thorne [16] next-to-leading order with EKS98 [17] shadowing corrections. The contribution to the continuum from semileptonic decay to muons of open charm pairs was estimated using PYTHIA [18], and a small correction, less than half the statistical uncertainties, was made for it in the SXF data set; but for the larger x_F data sets it is negligible and no corrections were made. In addition, a detailed construction of random muon pairs using single-muon events (which also provided a good fit to the like-sign muon mass spectra) was used to account for the smooth random background underneath the peaks. A maximum-likelihood method was used for fitting that took into account the statistical uncertainty of the data and of the Monte Carlo and randoms [19]. Figure 1 shows a typical fit to a mass spectrum using these components. Since the rates in the various detectors were nearly equal for the different targets, a correction for rate-dependent inefficiencies was not necessary.

We present our results in terms of α, where α is obtained by assuming the cross section dependence on nuclear mass, A, to be of the form $\sigma_A = \sigma_N \times A^\alpha$, where

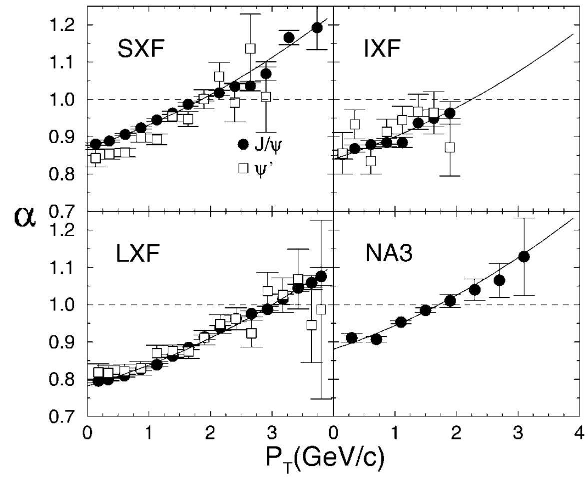

FIG. 2. α versus p_T for J/ψ (solid circles) and ψ' (open boxes) production by 800 GeV$/c$ protons. Results are shown for the three data sets [SXF, IXF, and LXF (see text)], which have $\langle x_F \rangle = 0.055$, 0.308, and 0.480, respectively. Only statistical uncertainties are shown. An additional systematic uncertainty of 0.5% is not included. Also shown are the NA3 results at 200 GeV$/c$ whose x_F range can be seen in Fig. 4. The solid curves represent the parametrization discussed in the text.

σ_N is the cross section on a nucleon. For the SXF data, α was obtained using Be and two different thickness W targets, while for the IXF and LXF data, Be, Fe, and W targets were used. The SXF data from the two W targets verified that no corrections for secondary production were

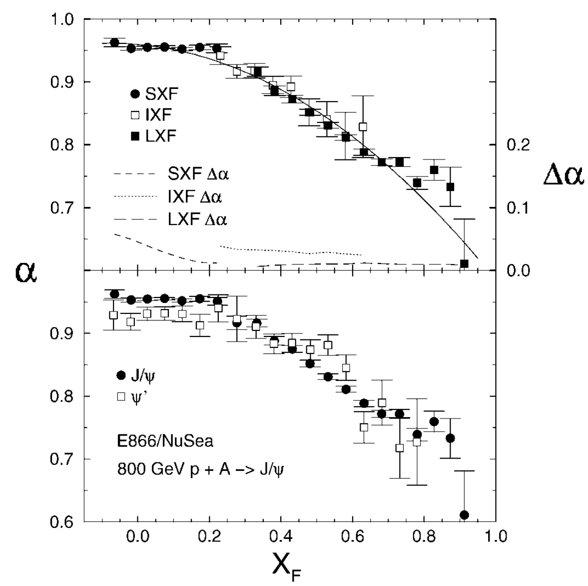

FIG. 3. α for J/ψ versus x_F for the three different data sets (top) and for J/ψ and ψ' after the data sets are combined (bottom). Values are corrected for the p_T acceptance, as discussed in the text. These corrections ($\Delta\alpha$) have a maximum value of 0.06 and are shown using the right-hand vertical scale in the top panel. The relative systematic uncertainty between α for J/ψ and ψ' is estimated to be 0.003, while the absolute systematic uncertainty is 0.01 in α; neither is included here. The solid curve represents the parametrization discussed in the text.

necessary. The p_T dependence of α is shown in Fig. 2, where we see essentially the same increase in α for all x_F ranges for both J/ψ and ψ', as well as for the 200 GeV/c NA3 data [4]. This increase is characteristic of multiple scattering of the incident parton and of the nascent $c\bar{c}$ in the final state. Note that for the IXF data the p_T acceptance is truncated at about 2 GeV/c because a more restrictive trigger was used.

Previous experiments such as E772 have had a limited acceptance in p_T which varied with x_F. Since the value of α depends strongly on p_T this can cause a distortion of the apparent shape of α versus x_F. The improvements in the E866/NuSea trigger allowed a much broader p_T acceptance than in these earlier measurements. However, for the lowest values of x_F at each spectrometer setting our p_T acceptance still becomes somewhat restricted. For the results presented here we have corrected the values of $\alpha(x_F)$ using a detailed simulation of our acceptance and a differential cross section shape versus p_T derived from our data.

The resulting dependence of α on x_F is shown in Fig. 3 and listed in Table I. The systematic uncertainty of 1% in the corrected α is dominated by the p_T acceptance correction. α for J/ψ is largest at values of x_F of 0.25 and below but strongly decreases at larger values of x_F. For ψ', α is smaller than for J/ψ for $x_F < 0.2$, remains relatively constant up to x_F of 0.5 (becoming slightly larger than for J/ψ), and then falls to values consistent with those for J/ψ for $x_F > 0.6$. The significance of the overall J/ψ, ψ' difference for $x_F < 0.2$ is about 4σ with respect to the statistical and relative systematic uncertainties. This difference is consistent with less accurate results obtained by NA38 for p-A at 450 GeV/c [6], but is inconsistent with the quoted NA38 result that also included the p-p and p-d data from NA51. Although slightly larger α values for ψ' than for J/ψ can be seen near $x_F = 0.55$, we should point out that if instead we emphasize the velocity of $c\bar{c}$ and plot α versus rapidity, then the agreement is quite good in this region. The reduced α at small x_F is also evident in Fig. 2 where α for ψ' falls consistently below that for J/ψ at low p_T for the SXF data set.

Our results for J/ψ α can be represented for convenience by the simple parametrizations shown as solid lines in Figs. 2 and 3: $\alpha(x_F) = 0.960(1 - 0.0519x_F - 0.338x_F^2)$, and $\alpha(p_T) = A_i(1 + 0.0604p_T + 0.0107p_T^2)$, where $A_i = 0.870$, 0.840, 0.782, and 0.881 for the SXF, IXF, and LXF data sets and for the NA3 data, respectively.

A comparison of our results with earlier data from E772 at 800 GeV/c [1] and also with NA3 at 200 GeV/c [4] is shown in Fig. 4. It illustrates that the suppression seen for J/ψ production scales with x_F but not with $p_{J/\psi}^{\mathrm{LAB}}$ above about 90 GeV/c, which corresponds to $x_F > 0.05$ for our data and to $x_F > 0.4$ for NA3. Also of interest in these figures is a comparison of our results with those of E772. At the small-x_F end of the E772 data their published results drop significantly below our results. As was discussed above, the E772 data have severe narrowing of the p_T acceptance for their smallest x_F bins, and a large correction that could easily bring the E772 points into agreement with our data is expected. Similar arguments hold for the E789 J/ψ data (not shown) at small to negative x_F [3], where we

TABLE I. α versus x_F [20] for J/ψ and ψ'. α is defined by $\sigma_A = \sigma_N \times A^\alpha$ and is equal to one if there is no suppression and the cross section scales simply as the number of nucleons. The average momentum fraction of the struck parton, x_2 [21], and the center-of-mass rapidity, $y_{\mathrm{c.m.}}$, are also shown. An additional systematic uncertainty of 1% is not included here.

$\langle x_F\rangle$	$\langle y_{\mathrm{c.m.}}\rangle_{J/\psi}$	$\langle x_2\rangle_{J/\psi}$	$\alpha_{J/\psi}$	$\langle y_{\mathrm{c.m.}}\rangle_{\psi'}$	$\langle x_2\rangle_{\psi'}$	$\alpha_{\psi'}$
−0.065	−0.390	0.1192	0.962(7)	−0.344	0.1346	0.929(24)
−0.019	−0.115	0.0902	0.953(3)	−0.104	0.1056	0.918(14)
0.027	0.161	0.0679	0.955(2)	0.132	0.0828	0.931(11)
0.075	0.433	0.0511	0.955(2)	0.369	0.0645	0.932(11)
0.124	0.680	0.0395	0.952(3)	0.588	0.0513	0.931(12)
0.173	0.896	0.0316	0.955(4)	0.785	0.0418	0.913(18)
0.223	1.091	0.0262	0.951(6)	0.974	0.0347	0.940(22)
0.277	1.288	0.0213	0.917(11)	1.144	0.0293	0.923(36)
0.332	1.427	0.0182	0.916(6)	1.281	0.0253	0.910(18)
0.381	1.551	0.0160	0.888(7)	1.401	0.0223	0.884(16)
0.431	1.663	0.0142	0.875(6)	1.512	0.0199	0.885(15)
0.481	1.764	0.0128	0.852(5)	1.614	0.0179	0.874(16)
0.531	1.858	0.0117	0.831(5)	1.705	0.0163	0.881(16)
0.582	1.945	0.0107	0.811(5)	1.791	0.0150	0.845(20)
0.632	2.026	0.009 84	0.789(6)	1.869	0.0138	0.751(25)
0.682	2.098	0.009 16	0.772(5)	1.942	0.0129	0.790(36)
0.732	2.166	0.008 55	0.772(7)	2.009	0.0120	0.718(49)
0.781	2.228	0.008 04	0.739(10)	2.071	0.0113	0.727(69)
0.828	2.286	0.007 60	0.760(17)			
0.873	2.338	0.007 23	0.733(32)			
0.913	2.383	0.006 98	0.611(71)			

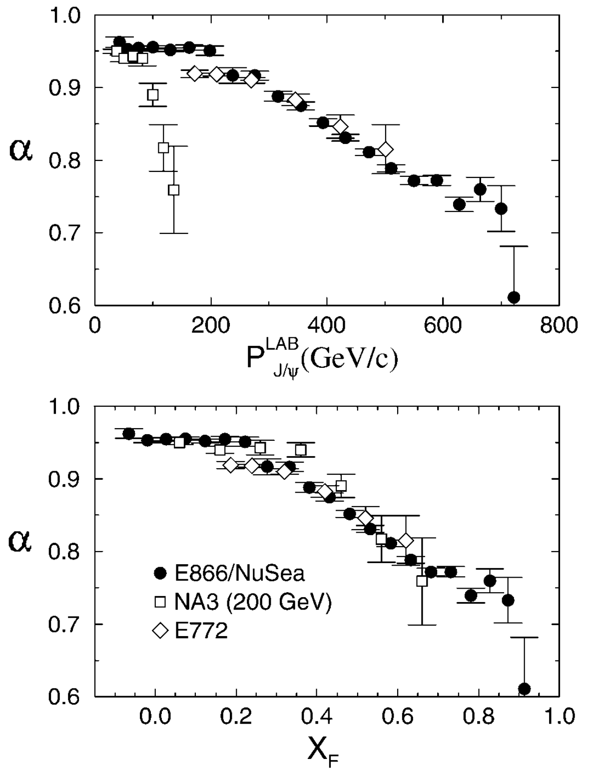

FIG. 4. α versus x_F and versus $p_{J/\psi}^{\mathrm{LAB}}$ for J/ψ from E866/NuSea (800 GeV/c) (solid circles) compared to E772 (open diamonds) and NA3 (200 GeV/c) (open squares) showing the scaling with x_F (bottom) and lack of scaling with $p_{J/\psi}^{\mathrm{LAB}}$ (top).

estimate about an 8% correction which would bring those results into agreement with ours. On the other hand, the large x_F results from E789 [2] appear to be high by more than their systematic uncertainty of 2.5%.

The suppression of J/ψ production near $x_F = 0$ is usually thought to be caused by absorption, the dissociation of the $c\bar{c}$ pair by interactions with the nucleus or comovers [8] into separate quarks that eventually hadronize into D mesons. This model is supported by both the increased suppression of the ψ' that we observe near $x_F = 0$ and the absence of suppression of D meson production in the same kinematic region [22]. At small x_F, the velocity of the $c\bar{c}$ pair is low enough that it may hadronize within the nucleus, so the larger ψ' would be absorbed more strongly [9,10]. However, the observed constancy of α for both J/ψ and ψ' up to $y_{\mathrm{c.m.}} \simeq 1$ complicates this interpretation since these models predict that faster $c\bar{c}$ pairs above $x_F \simeq 0.1$ would experience similar absorption, whether they eventually hadronize outside the nucleus into a J/ψ or a ψ'. At larger values of x_F, above 0.3, our data show similar suppression for J/ψ and ψ'. Furthermore, if absorption by the nuclear medium is the dominant suppression mechanism, the effect should scale with $p_{J/\psi}^{\mathrm{LAB}}$, but Fig. 4 shows that scaling breaks down in the middle of the region where we observe α to be constant.

Shadowing of the small-x target gluon distributions is also thought to play a role in the observed suppression, but current estimates [8,17] predict at most a few percent drop in $\alpha(x_F)$, even at the largest x_F values. Also, as is seen for our data (but not shown) and was seen previously [1], there is a lack of scaling with x_2, which is related to that shown above for $p_{J/\psi}^{\mathrm{LAB}}$ since $x_2 \propto 1/p_{J/\psi}^{\mathrm{LAB}}$. This appears to rule out large contributions from shadowing. Our studies [14] show that for Drell-Yan the dominant nuclear effect is shadowing of the antiquark distributions and that the energy loss of the incident quark is small. Although the incoming gluon's energy loss is expected to be larger by a color factor of 9/4 and the additional energy loss of the outgoing $c\bar{c}$ may be as large as that of a gluon, we still expect the overall contribution of energy loss to be small for resonance production.

In conclusion, we have presented new data for the suppression of J/ψ and ψ' production in heavy versus light nuclei for 800 GeV/c proton-nucleus collisions. The kinematic coverage in x_F (-0.10 to 0.93) and p_T (0–4 GeV/c) and statistical accuracy surpass that of previous experiments. Corrections are made to the data to account for the narrowing p_T acceptance at the smaller values of x_F. The largest value of α (integrated over p_T) of about 0.95 is seen at x_F near 0.25 and below with strongly falling values for larger x_F. The most striking new result is that the suppression for the ψ' is stronger than that for J/ψ at x_F near zero.

We thank Ramona Vogt and Boris Kopeliovich for many useful discussions and the Fermilab Particle Physics, Beams and Computing Divisions for their assistance. This work was supported in part by the U.S. Department of Energy.

*Present address: University of Illinois, Urbana, IL 61801.
†On leave from Kurchatov Institute, Moscow, Russia.

[1] D. M. Alde *et al.*, Phys. Rev. Lett. **66**, 133 (1991); **66**, 2285 (1991).
[2] M. S. Kowitt *et al.*, Phys. Rev. Lett. **72**, 1318 (1994).
[3] M. J. Leitch *et al.*, Phys. Rev. D **52**, 4251 (1995).
[4] J. Badier *et al.*, Z. Phys. C **20**, 101 (1983).
[5] M. J. Corden *et al.*, Phys. Lett. **110B**, 415 (1982).
[6] M. C. Abreu *et al.*, Phys. Lett. B **444**, 516 (1998).
[7] M. C. Abreu *et al.*, Phys. Lett. B **450**, 456 (1999).
[8] R. Vogt, hep-ph/9907317; R. Vogt, S. J. Brodsky, and P. Hoyer, Nucl. Phys. **B360**, 67 (1991).
[9] F. Arleo, P.-B. Gossiaux, T. Gousset, and J. Aichelin, hep-ph/9907286.
[10] L. Gerland, L. Frankfurt, M. Strikman, H. Stöcker, and W. Greiner, nucl-th/9908052.
[11] Y. B. He, J. Hüfner, and B. Z. Kopeliovich, hep-ph/9908243.
[12] J. A. Crittenden *et al.*, Phys. Rev. D **34**, 2584 (1986).
[13] C. A. Gagliardi *et al.*, Nucl. Instrum. Methods Phys. Res., Sect. A **418**, 322 (1998).
[14] M. A. Vasiliev *et al.*, Phys. Rev. Lett. **83**, 2304 (1999).
[15] E. A. Hawker *et al.*, Phys. Rev. Lett. **80**, 3715 (1998).
[16] A. D. Martin, R. G. Roberts, W. J. Stirling, and R. S. Thorne, Eur. Phys. J. C **4**, 463 (1998).

[17] K. J. Eskola, V. J. Kolhinen, and C. A. Salgado, Eur. Phys. J. C **9**, 61 (1999).
[18] H.-U. Bengtsson and T. Sjöstrand, Comput. Phys. Commun. **46**, 43 (1987).
[19] The HMCMLL fitting routine from CERNLIB, R. Barlow and C. Beeston, Comput. Phys. Commun. **77**, 219 (1993).
[20] We calculate $x_F = p_L^{CM}/(\sqrt{s}/2)$, neglecting a small $(1 - \tau \simeq 0.6\%)$ correction for the J/ψ mass.
[21] We calculate x_2 by ignoring the soft gluon that accompanies the $c\bar{c}$ pair in the final state in the same way one would calculate x_2 for the leading-order Drell-Yan process.
[22] M. J. Leitch *et al.*, Phys. Rev. Lett. **72**, 2542 (1994).